# Potential of Optical Frequency Domain Imaging for Differentiation Between Early and Advanced Coronary Atherosclerosis

**Takahiro Imanaka**
Hyogo College of Medicine https://orcid.org/0000-0002-7538-1296
**Kenichi Fujii** ( fujiik@hirakata.kmu.ac.jp )
Hyogo College of Medicine
**Takamasa Tanaka**
Hyogo College of Medicine
**Koji Yanaka**
Hyogo College of Medicine
**Toshio Kimura**
Hyogo College of medicine
**Nagataka Yoshihara**
Hyogo College of Medicine
**Kojiro Miki**
Hyogo College of Medicine
**Kenji Kawai**
Hyogo College of Medicine
**Hirokuni Akahori**
Hyogo College of Medicine
**Rika Kawakami**
Hyogo College of Medicine
**Hiroyuki Hao**
Nihon University School of Medicine
**Seiichi Hirota**
Hyogo College of Medicine
**Masaharu Ishihara**
Hyogo College of Medicine

**Research Article**

**Keywords:** atherosclerosis, optical coherence tomography, coronary artery disease, histopathology

**Posted Date:** November 23rd, 2021

**DOI:** https://doi.org/10.21203/rs.3.rs-1015982/v1

## Abstract

# Purpose

Optical frequency domain imaging (OFDI) is widely used to characterize lipidic-atherosclerotic plaques, shown as signal-poor regions with diffuse borders, in clinical setting. Given that lipid components are common to both fibroatheroma (FA) and pathological intimal thickening (PIT), it is unclear whether OFDI can be used to accurately distinguish between FA and PIT. This study evaluated the differences in OFDI findings between FA and PIT in comparison with histopathology.

# Methods

A total of 631 histological cross-sections from 14 autopsy hearts were analyzed for the comparison between OFDI and histological images. Of those, 190 (30%) sections were diagnosed with PIT and 120 (19%) with FA. All OFDI images were matched with histology and the OFDI signal attenuation rate was calculated from an exponential. The lipid length was measured longitudinally, and the lipid arc was measured with a protractor centered in the center of the lumen.

# Results

There was no significant difference in the OFDI signal attenuation rate between FA and PIT (3.09 ± 1.04 versus 2.79 ± 1.20, p = 0.13). However, the lipid length was significantly longer and the maximum lipid arc was significantly larger in FA than in PIT (7.5 [4.3–10.3] mm versus 4.3 [2.7–5.8] mm, p < 0.0001, and 125 [101–174]° versus 96 [74–131]°, p < 0.0001, respectively).

# Conclusions

OFDI may be capable of discriminating advanced lipid plaques from early stage atherosclerosis based on the longitudinal and circumferential extent of signal-poor region.

## Introduction

Over the decades, atherosclerosis of human coronary artery progresses in stages, with early atherosclerotic lesion developing into advanced stage lesion, under the influence of various factors. Pathologic intimal thickening (PIT) is founded in an early stage of human coronary atherosclerotic lesion[1]. PIT is characterized by presence of an extracellular lipid pool with co-existing smooth muscle cell remnant is observed close to medial wall and various degrees of macrophage infiltration, that is located close to the lumen[2]. In contrast, fibroatheroma (FA) is a progressive stage of atherosclerotic lesion. FA is characterized by presence of necrotic core, which is characterized by discrete collections of cellular debris

and cholesterol crystal, and is distinguished from PIT lesions by the presence of a necrotic core[3]. Notably, thin-cap FA, referring to as a vulnerable plaque, is a precursor lesion of plaque rupture and may lead to acute coronary syndrome. Therefore, differentiating FA from PIT is clinically important.

Optimal coherence tomography (OCT) and optical frequency domain imaging (OFDI) are light-based imaging devices that can clearly visualize various morphological features of coronary arteries[4]. Based on optical properties, OCT is able to distinguish different tissue types, such as fibrous, lipid-rich, necrotic, or calcified tissue[5]. Lipid-rich plaques on OCT images are visualized as a signal-poor region with a diffuse border due to multiple scattering in lipids at light wavelengths of approximately 1,000 nm [5]. Given that lipid components are common to both FA and PIT, it is unclear whether OCT can be used to accurately distinguish between FA and PIT. Therefore, in the current study, we analyzed the differences in OFDI findings between FA and PIT in comparison with histopathology.

# Methods

### Study subject

Thirty-nine coronary arteries from 14 human cadaver hearts were analyzed for the comparison between OFDI and histological images. All three major coronary arteries were collected from 11 patients, whereas only two major coronary arteries were collected from three patients due to hypoplasia of the coronary arteries. The cause of death was cardiovascular disease in seven cadavers, non-cardiac-related in six cadavers, and unknown in the remaining one cadaver. The experimental study protocol was approved by the Institutional Review Board of Hyogo College of Medicine (approval number 3766).

### OFDI imaging procedure

Three major coronary arteries, including the left anterior descending artery, the circumflex artery, and the right coronary artery with the surrounding fatty tissue, were carefully removed from the autopsy hearts after death for ex vivo OFDI imaging. The surrounding fatty tissue was carefully dissected from each coronary specimen. Before OFDI examination, using a tapered surgical needle, multiple 6-0 proline sutures were carefully inserted into the plaque segment as a reference point for matching between the OFDI and histological images. This method was successfully performed in previous comparative studies that compared histological findings and IVUS images[6,7]. A 0.014-inch guidewire was advanced to the distal end of each harvested major coronary artery, followed by an OFDI catheter (LUNAWAVE, Terumo Corporation, Tokyo, Japan). OFDI images of the entire vessel were acquired at a pullback rate of 20 mm/s (160 frames/s).

### Histopathological preparation and assessment

After OFDI examination, each coronary artery was fixed in 10% neutral buffered formalin for 48 h. The ring-like arterial specimens obtained at the same level as the imaging study were decalcified for 5 h, before being embedded in paraffin and cut every 3 mm into 4-μm transverse sections perpendicular to the

longitudinal axis of the artery. All histological sections were stained with hematoxylin & eosin, elastic van Gieson, and Masson's trichrome stain. Coronary plaques were classified using the modified American Heart Association classification[2] into the following categories: Adaptive intimal thickening, defined as lesions with predominantly fibrous tissue and no macrophage and lipid pool; PIT, defined as lesions with lipid pools and no apparent necrosis; FA, defined as lesions comprised of lipid pools and necrotic cores, including cholesterol clefts and cellular debris with an overlying fibrous cap; fibrocalcific plaque, defined as lesions with calcification and absence or fractions of a necrotic core; and healed plaque, defined as lesions composed of smooth muscle cells, proteoglycans, and collagen type III, with or without an underlying disrupted fibrous cap and necrotic core. Histological assessment of each cross-section was performed by a single experienced pathologist (R.K.) who was blinded to the OFDI findings.

### Co-registration of OFDI images with histology

All OFDI images were co-registered with histologic sections by an experienced investigator. Adjustments were made using the sutures and luminal configuration or anatomical landmarks such as vessel branches, thus improving the accuracy of registration. A total of 228 histological segments were excluded due to difficulties with co-registration. Finally, 631 pairs of matched images were acquired from OFDI with corresponding histological sections.

### Quantitative OFDI analysis

OFDI image analysis was performed only when histological cross-sections of paired images were classified as a FA or PIT. An OFDI-derived lipid image was defined as a diffusely bordered, signal-poor region[8, 9]. OFDI was reviewed longitudinally, and the lipid length was measured by detection of sequential OFDI frames within a plaque segment containing lipids. The lipid arc measurements were made by defining the circumferential extent of the lipidic tissue from the lumen center at the cross-section of minimum lumen area (Figure 1). The OFDI signal intensity was calculated on each corresponding OFDI cross-section using Image J software (National Institutes of Health, Rockville, Maryland, USA). Because the OFDI signal intensity of lipid tissue should gradually decrease from the surface to the inside, the attenuation of lipid signal intensity was analyzed by fitting it to a single exponential function: $y = A \times \exp^{-Bx}$, where index B represents an "attenuation rate" (Figure 2). OFDI images were analyzed by an experienced observer (T.I.) who was blinded to the clinical and histopathological presentations.

### Statistical analysis

Continuous variables are expressed as mean ± standard deviation or median (Q1–Q3). The normality of the distribution was analyzed using the Shapiro–Wilk test, and homoscedasticity was analyzed using the Bartlett test. Continuous variables were compared using Student's t-test or Wilcoxon rank sum test. The area under the receiver operating characteristic (ROC) curve was evaluated to determine the best cutoff of lipid length and the FA angle. P-values < 0.05 were considered statistically significant. Statistical analyses were performed with the use of JMP Pro 14.2.0 (SAS Institute Inc., Cary, NC, USA).

## Results

On histological evaluation of 631 matched cross-sections, 208 (33%) sections were diagnosed with adaptive intimal thickening, 190 (30%) with PIT, 120 (19%) with FA, 104 (17%) as fibrocalcific, and 9 (1%) as healed plaque according to the modified AHA classification.

# Quantitative Ofdi Analysis

All cross sectional images of both PIT and FA showed low intensity area with diffuse border. There was no significant difference in the optical attenuation coefficient between FA and PIT (3.09 ± 1.04 versus 2.79 ± 1.20, p = 0.13) (Figure 3A). However, the lipid length was significantly longer in FA than in PIT (7.5 [4.3–10.3] mm versus 4.3 [2.7–5.8] mm, p < 0.0001) (Figure 3B). ROC analysis identified 5.8 mm as the optimal cutoff point for prediction of the lipid length of FA (sensitivity, 66% and specificity, 74%; area under the curve, 0.73; p < 0.0001) (Figure 4A). Furthermore, the maximum lipid arc was significantly larger in FA than in PIT (125 [101–174]° versus 96 [74–131]°, p < 0.0001] (Figure 3C). ROC analysis identified 113° as the optimal cutoff point for prediction of the maximum FA angle (sensitivity, 70% and specificity, 68%; area under the curve, 0.71; p < 0.0001) (Figure 4B). Representative images of FA and PIT are shown in Figure 5.

## Discussion

The main findings of this study are as follows: 1) the lipid length was significantly longer and the maximum lipid arc was significantly larger in FA than in PIT, and 2) the OFDI signal attenuation rate was similar between FA and PIT. To the best of our knowledge, this is the first study to report the differences in OFDI findings between “lipids” at an early stage and those at an advanced stage, in comparison with histopathology.

OFDI is accepted as a high-resolution intracoronary imaging modality to assess morphological features of native coronary arteries in comparison with other imaging modalities[10, 11]. Given that it is recognized that OFDI is capable of differentiating lipid tissue from fibrous and calcific tissue, OFDI is widely used as a promising imaging modality for identifying vulnerable plaques in clinical settings. Pathologic features of vulnerable plaques are characterized by a large necrotic core with an overlying thinner fibrous cap[1, 12]. Moreover, on OFDI, lipidic tissues appear as signal-poor regions with diffuse borders because of multiple scattering in lipids at light wavelengths of approximately 1000 nm[13]. A previous ex vivo imaging study validated this finding with ex vivo OCT imaging of diseased atherosclerotic arterial segments obtained at autopsy, and reported a sensitivity and specificity of 90–94% and 90–92% for lipidic plaques, respectively[5]. This finding was confirmed by another ex vivo study that showed > 90% sensitivity and specificity for identifying lipidic plaques by OCT in 40 human cadavers[14]. However, there is a pitfall in the diagnosis of lipidic plaques by OFDI in that the OFDI signal could be attenuated because of multiple scattering, not only in the necrotic core, but also in any lipid components, because of the features of near-

infrared light. Therefore, we previously reported that the diagnostic accuracy of OCT for characterizing thin-cap FA, using histology as a standard, was only 41%[15]. The majority of tissue, falsely diagnosed as thin-cap fibroatheroma on OCT, was categorized as PIT. In line with our findings, a previous study showed that CD68-stained dense foam cell infiltration creates a highly scattered layer that casts a dark shadow on the tissue behind, and therefore appears as a thin-cap FA[16]. In the current study, PIT without a necrotic core, which was considered as early-stage atherosclerosis, appeared as a low-signal-intensity tissue with diffusely delineated borders due to strong signal attenuation on OFDI. When the tissue contained a lipid component, the attenuation coefficient of the OFDI light signal was similar regardless of the presence of a necrotic core. These results are supported by a previous ex vivo OCT that showed a similar index of plaque attenuation of OCT signal between FA and PIT[17]. Because the necrotic core and other lipid components have similar OFDI attenuation coefficients, it remains difficult to distinguish between PIT and FA on a single cross-sectional OFDI image in vivo.

In the current study, we found that FA had a significantly longer and larger arc of low signal intensity area on OFDI compared to PIT. To date, there are no histopathological data investigating the size of lipid components in FA and PIT. However, PIT is considered a progressive lesion in the early stages of atherosclerosis and represents a precursor lesion to FA[1, 18]. Therefore, if PIT is a precursor lesion of FA, it is reasonable to assume that FA contains more lipid components than PIT. A previous clinical study has reported that the length of the lipid pool estimated by OCT was significantly longer in lesions with ≥ 50% ST resolution than in lesions with < 50% ST resolution[19]. Furthermore, another OCT study revealed a linear relationship between the intrastent protrusion area and the lipid index, which was calculated as the lipid arc multiplied by the lipid length[20]. These clinical data may support our finding that FA contained a larger amount of lipid components than PIT. Given the difficulty in differentiating FA from PIT, OFDI observers could misclassify PIT as a vulnerable plaque by only looking at a single cross-section of the OFDI image. The misclassification of plaque morphology in the catheterization laboratory may cause a treatment strategy to be selected, such as the use of an embolic protection device during percutaneous coronary intervention. Therefore, interventional cardiologists who are responsible for the interpretation of OFDI imaging should evaluate plaque morphology by looking at the entire segment, not just a single cross-section.

# Limitation

There were several limitations in the current study. First, the study was performed in a limited number of samples and therefore further investigations must be performed with larger samples to confirm the conclusions. Second, a lack of cardiac motion may have affected the OFDI images acquired ex vivo. Third, a positional discrepancy both OFDI images and histological cross-sections may have influenced the results. Therefore, utmost care was taken to ensure that OFDI images matched the histology. Finally, immunochemical staining to identify macrophages was not performed in the present study.

# Conclusion

This study revealed OFDI has the potential capability for discriminating advanced lipid plaques from early stage atherosclerosis based on the longitudinal and circumferential extent of signal-poor lipid plaque.

# Declarations


### Acknowledgments

The authors thank the staffs in the Department of Surgical Pathology at Hyogo College of Medicine for their excellent assistance for the study.

### Funding

This research did not receive any specific grant from funding agencies in the public, commercial, or not-for-profit sectors.



### Author information

Department of Cardiovascular and Renal Medicine, Hyogo College of Medicine, Hyogo, Japan

Takahiro Imanaka, Takamasa Tanaka, Koji Yanaka, Toshio Kimura, Nagataka Yoshihara, Kojiro Miki, Kenji Kawai, Hirokuni Akahori, Masaharu Ishihara

Division of Surgical Pathology, Hyogo College of Medicine, Hyogo, Japan

Kenichi Fujii, Rika Kawakami, Seiichi Hirota

Division of Human Pathology, Department of Pathology and Microbiology, Nihon University School of Medicine, Tokyo, Japan

Hiroyuki Hao

### Corresponding author

Correspondence to Kenichi Fujii


### Ethics declarations

### Conflict of intrest

Takahiro Imanaka has nothing to declare for this study. Masaharu Ishihara received research fund from Amgen Inc. (Japan), and lecture fees from Bayer Yakuhin, Ltd. (Japan), Daiichi Sankyo Company (Japan), Nippon Boehringer Ingelheim Co., Ltd. (Japan), and Otsuka Pharmaceutical Co., Ltd. (Japan), and scholarship funds from Abbott Co.,Ltd. (Japan), Otsuka Pharmaceutical Co.,Ltd. (Japan), MID,Inc. (Japan), Ono Pharmaceutical Co.,Ltd. (Japan), Orbusneich Medical K. K. (Japan), Kowa Pharmaceutical

Co.,Ltd. (Japan), Mitsubishi Tanabe Pharma Corporation (Japan), Terumo Corporation (Japan), Nipro Corporation (Japan), Lifeline Co.,Ltd. (Japan), Bayer Yakuhin, Ltd. (Japan), Fukuda Denshi Co.,Ltd. (Japan), and Boston Scientific K.K. (Japan), and endowed departments from Abbott (Japan), Medtronic Japan Co., Ltd. (Japan), and Nippon Boehringer Ingelheim Co., Ltd. (Japan). No other potential conflicts of interest relating to this article were reported.

### Ethical approval

The study protocol was approved by the Institutional Review Board of Hyogo College of Medicine (approval number 3766).

# References


1. Virmani R, Kolodgie FD, Burke AP, Farb A, Schwartz SM (2000) Lessons from sudden coronary death: a comprehensive morphological classification scheme for atherosclerotic lesions. Arterioscler Thromb Vasc Biol 20:1262–1275
2. Yahagi K, Kolodgie FD, Otsuka F, Finn AV, Davis HR, Joner M et al (2016) Pathophysiology of native coronary, vein graft, and in-stent atherosclerosis. Nat Rev Cardiol 13:79–98
3. Stary HC, Blankenhorn DH, Chandler AB, Glagov S, Insull W, Richardson M et al (1992) A definition of the intima of human arteries and of its atherosclerosis-prone regions. A report from the Committee on Vascular Lesions of the Council on Arteriosclerosis, American Heart Association. Circulation 85:391–405
4. Brezinski ME, Tearney GJ, Bouma BE, Izatt JA, Hee MR, Swanson EA et al (1996) Optical coherence tomography for optical biopsy. Properties and demonstration of vascular pathology. Circulation 93:1206–1213
5. Yabushita H, Bouma BE, Houser SL, Aretz HT, Jang IK, Schlendorf KH et al (2002) Characterization of human atherosclerosis by optical coherence tomography. Circulation 106:1640–1645
6. Kawasaki M, Takatsu H, Noda T, Ito Y, Kunishima A, Arai M et al (2001) Noninvasive quantitative tissue characterization and two-dimensional color-coded map of human atherosclerotic lesions using ultrasound integrated backscatter: comparison between histology and integrated backscatter images. J Am Coll Cardiol 38:486–492
7. Okubo M, Kawasaki M, Ishihara Y, Takeyama U, Kubota T, Yamaki T et al (2008) Development of integrated backscatter intravascular ultrasound for tissue characterization of coronary plaques. Ultrasound Med Biol 34:655–663
8. Fujii K, Kubo T, Otake H, Nakazawa G, Sonoda S, Hibi K et al (2020) Expert consensus statement for quantitative measurement and morphological assessment of optical coherence tomography. Cardiovasc Interv Ther 35:13–18
9. Tearney GJ, Regar E, Akasaka T, Adriaenssens T, Barlis P, Bezerra HG et al (2012) Consensus standards for acquisition, measurement, and reporting of intravascular optical coherence

tomography studies: a report from the International Working Group for Intravascular Optical Coherence Tomography Standardization and Validation. J Am Coll Cardiol 59:1058–1072

10. Jang IK, Bouma BE, Kang DH, Park SJ, Park SW, Seung KB et al (2002) Visualization of coronary atherosclerotic plaques in patients using optical coherence tomography: comparison with intravascular ultrasound. J Am Coll Cardiol 39:604–609
11. Sonoda S, Hibi K, Okura H, Fujii K, Honda Y, Kobayashi Y (2020) Current clinical use of intravascular ultrasound imaging to guide percutaneous coronary interventions. Cardiovasc Interv Ther 35:30–36
12. Otsuka F, Joner M, Prati F, Virmani R, Narula J (2014) Clinical classification of plaque morphology in coronary disease. Nat Rev Cardiol 11:379–389
13. Allen TJ, Hall A, Dhillon AP, Owen JS, Beard PC (2012) Spectroscopic photoacoustic imaging of lipid-rich plaques in the human aorta in the 740 to 1400 nm wavelength range. J Biomed Opt 17:061209
14. Kume T, Akasaka T, Kawamoto T, Watanabe N, Toyota E, Neishi Y et al (2006) Assessment of coronary arterial plaque by optical coherence tomography. Am J Cardiol 97:1172–1175
15. Fujii K, Hao H, Shibuya M, Imanaka T, Fukunaga M, Miki K et al (2015) Accuracy of OCT, grayscale IVUS, and their combination for the diagnosis of coronary TCFA: an ex vivo validation study. JACC Cardiovasc Imaging 8:451–460
16. van Soest G, Regar E, Goderie TP, Gonzalo N, Koljenović S, van Leenders GJ et al (2011) Pitfalls in plaque characterization by OCT: image artifacts in native coronary arteries. JACC Cardiovasc Imaging 4:810–813
17. Gnanadesigan M, Hussain AS, White S, Scoltock S, Baumbach A, van der Steen AF et al (2017) Optical coherence tomography attenuation imaging for lipid core detection: an ex-vivo validation study. Int J Cardiovasc Imaging 33:5–11
18. Kolodgie FD, Burke AP, Nakazawa G, Virmani R (2007) Is pathologic intimal thickening the key to understanding early plaque progression in human atherosclerotic disease? Arterioscler Thromb Vasc Biol 27:986–989
19. Ikenaga H, Ishihara M, Inoue I, Kawagoe T, Shimatani Y, Miura F et al (2013) Longitudinal extent of lipid pool assessed by optical coherence tomography predicts microvascular no-reflow after primary percutaneous coronary intervention for ST-segment elevation myocardial infarction. J Cardiol 62:71–76
20. Uzu K, Shinke T, Otake H, Takaya T, Osue T, Iwasaki M et al (2017) Morphological and pharmacological determinants of peri-procedural myocardial infarction following elective stent implantation: Optical coherence tomography sub-analysis of the PRASFIT-Elective study. J Cardiol 70:545–552

# Figures

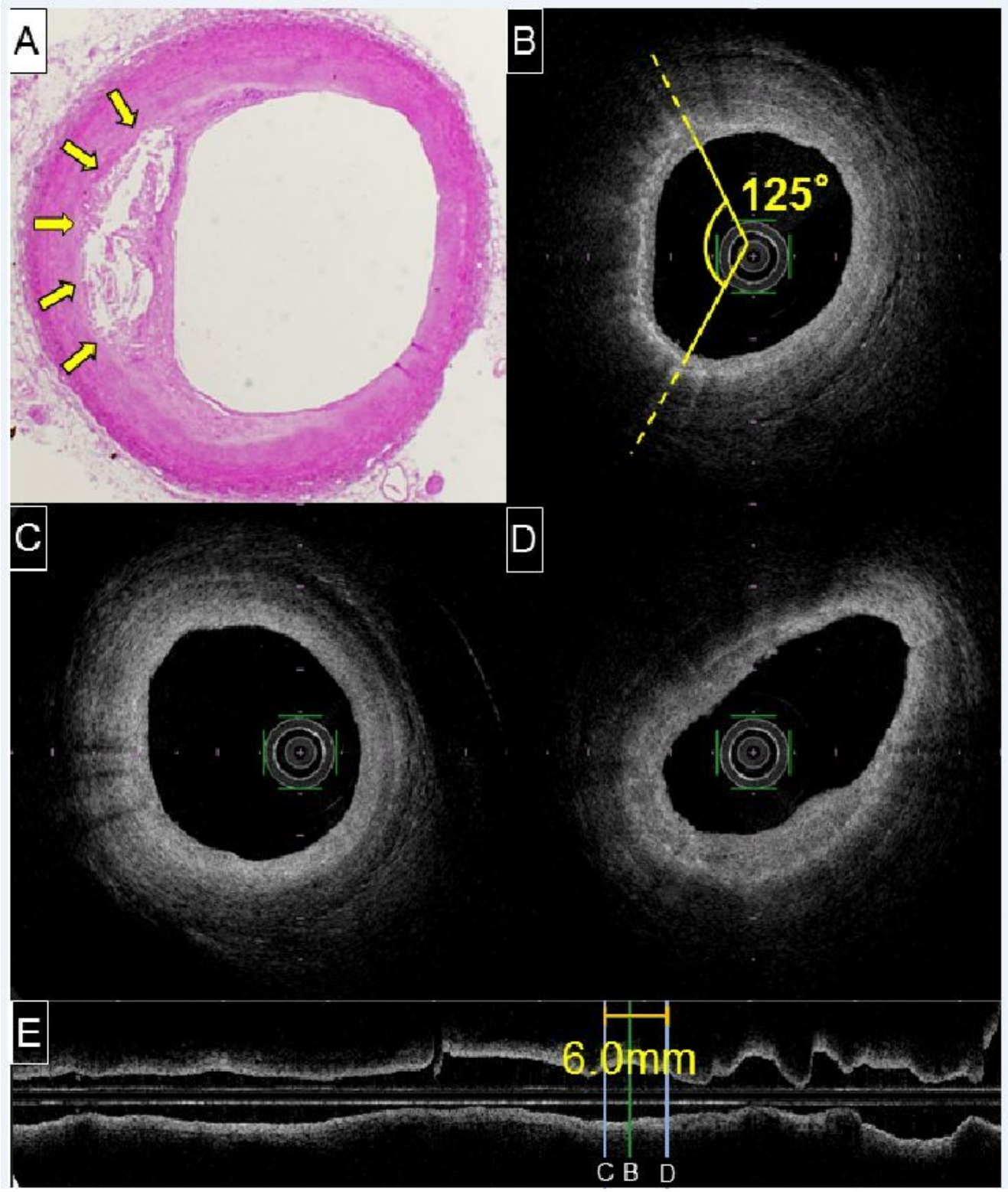


**Figure 1**

Measurement of lipid length and maximum lipid angle (A) A histopathological cross-section showing necrotic core formation within the plaque (arrows) (hematoxylin & eosin; scale bar = 1000 μm). (B) A corresponding OFDI image from the same area in A showing a low signal intensity area. The angle of low signal intensity area was 125°. The lipid lesion was defined as a lesion consisting of serial OFDI images showing low signal intensity areas with diffuse borders. OFDI images showing a distal edge of the lipid

lesion (C) and a proximal edge of the lipid lesion (D). (E) The length of the lipid lesion was 6.0 mm. OFDI = optical frequency domain imaging

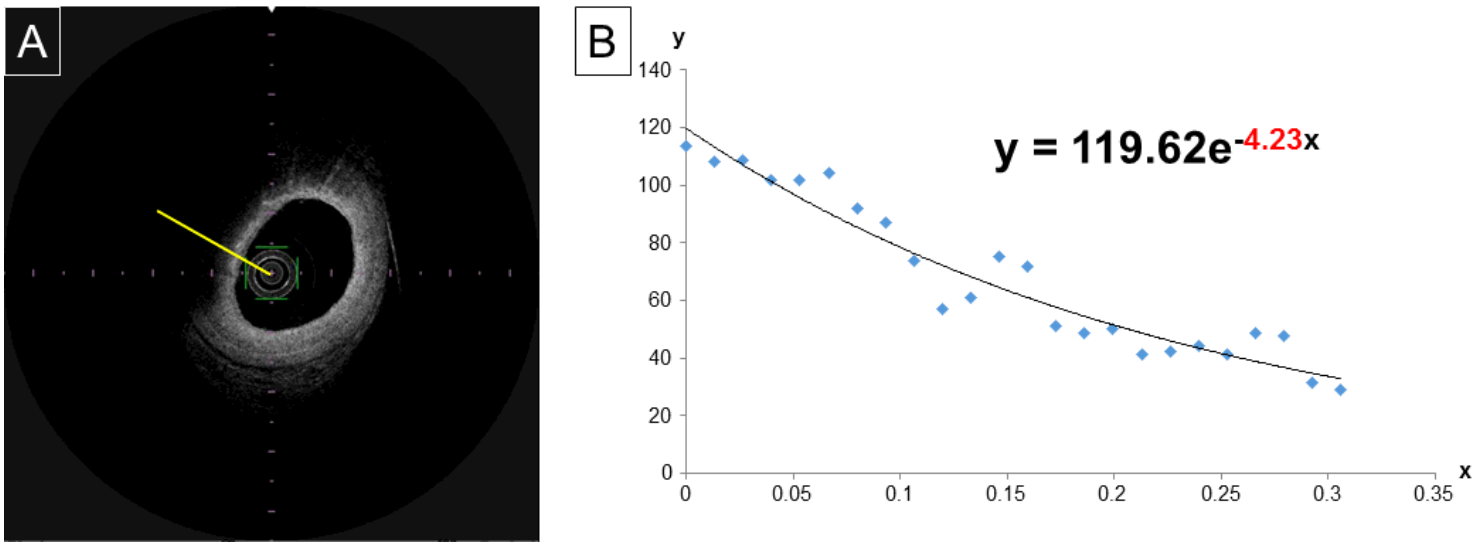


## Figure 2

Measurement method of optical attenuation coefficient (A) OFDI image showing a low signal intensity area with a diffuse border. (B) The OFDI signal intensity was calculated from the luminal surface by Image J software, and fitted to the following approximate formula: y = A × exp −Bx. Index B reflects an “attenuation rate”. This index rate was defined as an optical attenuation coefficient. The OFDI signal attenuation rate measured from the luminal surface to the leading edge of the outer lumen was 4.23. OFDI = optical frequency domain imaging

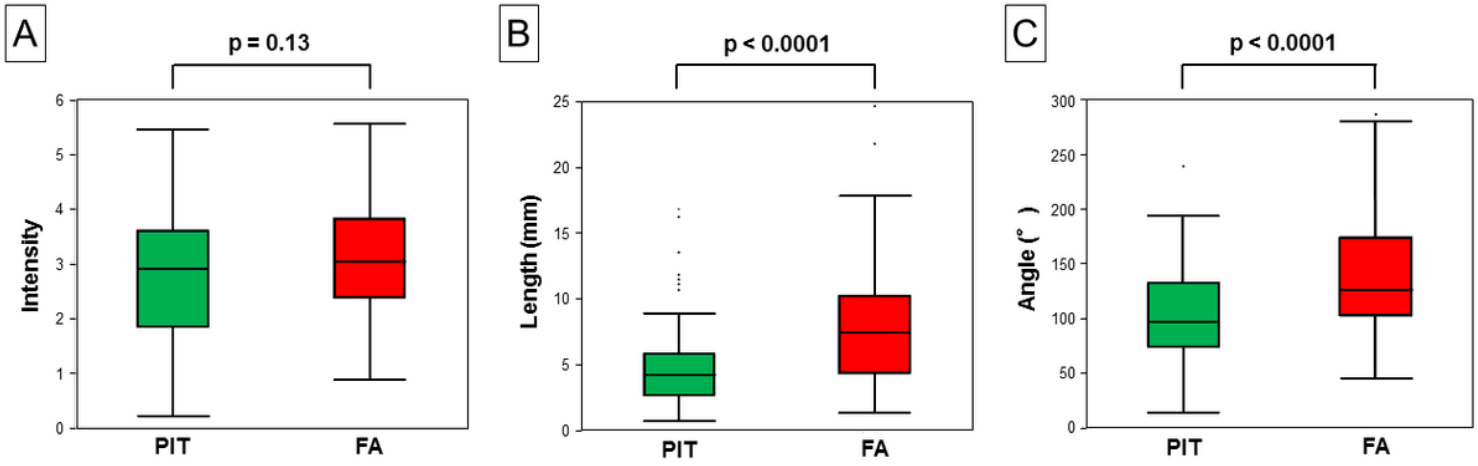


## Figure 3

Optical attenuation coefficients, lipid length, and maximum lipid arc of PIT and FA (A) There was no significant difference in optical attenuation coefficient between the two groups. (B) The lipid length was significantly longer in FA than in PIT. (C) The maximum lipid arc was significantly larger in FA compared to PIT. FA = fibrous cap atheroma; PIT = pathological intimal thickening

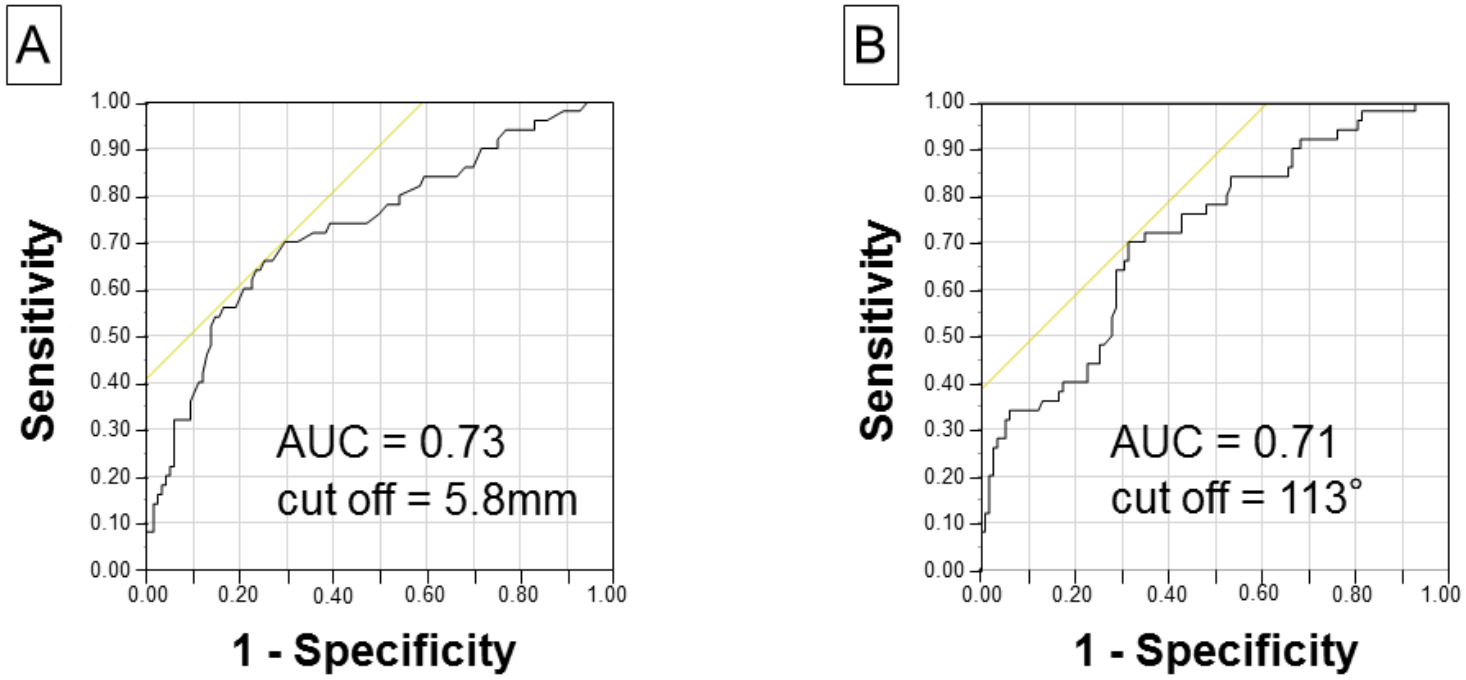


**Figure 4**

ROC and area under the curve for predicting the presence of FA (A) ROC analysis of the lipid length of FA. (B) ROC analysis of the lipid arc of FA. ROC = receiver operating characteristic; FA = fibrous cap atheroma

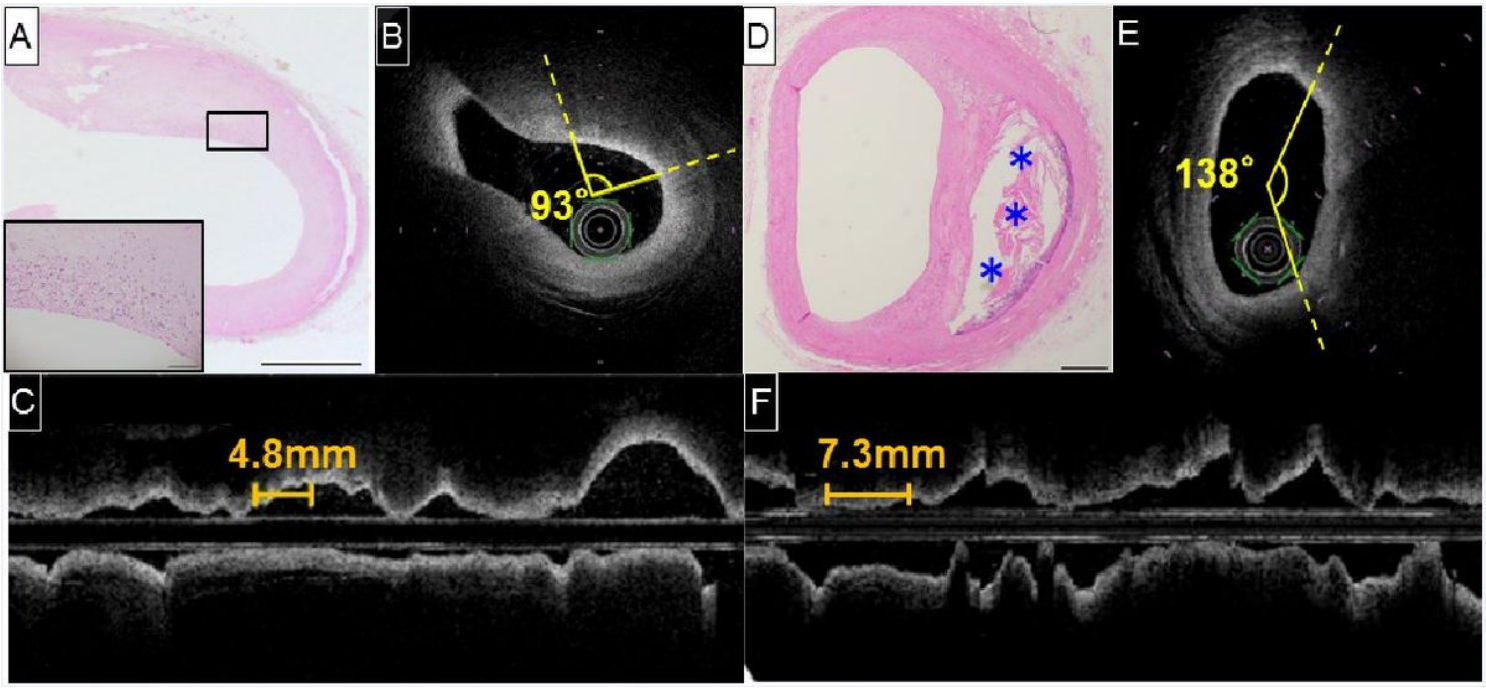


**Figure 5**

Representative images of PIT and FA (A) Histopathological cross-section of PIT (hematoxylin & eosin; scale bar = 1000 μm). A magnified image of the boxed area in A the accumulation of foam cells (hematoxylin & eosin; scale bar = 100 μm). (B) A corresponding OFDI image from the same area in A showing a low signal intensity area. The maximum angle was 93°. (C) The lipid length was 4.8 mm. (D)

Histopathological cross section of a FA (hematoxylin & eosin; scale bar = 1000 μm) showing a necrotic core (asterisks). (E) A corresponding OFDI image from the same area in E showing a large low signal intensity area. The maximum angle was 138°. (F) The lipid length was 7.3 mm, which was longer than that in PIT. PIT = pathological intimal thickening; FA = fibrous cap atheroma; OFDI = optical frequency domain imaging